

High-power supercontinuum generation in dielectric-coated metallic hollow waveguides

A. Husakou* and J. Herrmann

Max Born Institute of Nonlinear Optics and Short Pulse Spectroscopy, Max Born Str 2a, D-12489 Berlin, Germany

(Dated: February 12, 2022)

In this Letter we theoretically study a novel approach for soliton-induced supercontinuum generation based on the application of metallic dielectric-coated hollow waveguides. The low loss of such waveguides permits the use of smaller diameters with enhanced dispersion control and enables the generation of two-octave-broad spectra with unprecedentedly high spectral peak power densities up to five orders of magnitude larger than in standard PCFs with high coherence. We also predict that high-power supercontinua in the vacuum ultraviolet can be generated in such waveguides.

PACS numbers: 42.65.Re, 42.65.Tg

It is well known that lasers generate strongly directed coherent light with the highest possible brightness. However, a typical laser is a quasi-monochromatic source emitting light of only one color. Many applications require light sources which share with a laser its unidirectional and coherent properties but span the whole spectral range of a rainbow like the sun or an electric bulb. The latter sources, however, are unable to emit coherent, unidirectional and bright radiation.

A milestone on the way towards a coherent white-light high-brightness source (supercontinuum, SC) was achieved by the application of photonic crystal fibres (PCF) [1, 2]. When a femtosecond pulse with only nJ energy from a laser oscillator is focused into such fiber, a dramatic conversion from narrow band light to two-octaves-broad spectra was observed [3]. The discovery of SC generation in PCFs encouraged extensive research activities (see e.g. Refs.[4, 5, 6, 7, 8, 9, 10, 11]) and is now considered to be one of the leading-edge research areas in photonics. This coherent white-light source is applied in physics, chemistry, biology, telecommunication and medicine using numerous methods ranging from the frequency comb method [12, 13], optical coherence tomography [14], absorption spectroscopy[15], and flow cytometry to WDM in telecommunication and others. There are now a few commercial suppliers for these purposes (see e.g. [16]).

Supercontinuum generation in PCFs is based on an effect for spectral broadening [4] which differ from the main previously known mechanism for spectral broadening by self-phase modulation. It is connected with the soliton dynamics in the anomalous dispersion region of the PCFs. The high refractive-index contrast in PCFs leads to a shift of the zero dispersion wavelength to the visible and anomalous dispersion at the wavelength of typical lasers, such as a Ti:sapphire laser. Therefore the input pulse splits into several fundamental solitons with different amplitudes and distinct red-shifted input frequencies. Per definition, a fundamental soliton does not change its energy, however if it is perturbed by third- and higher-order dispersion of the fibre it can emit blue-

shifted nonsolitonic radiation (also known as dispersive radiation) at a wavelength determined by phase matching [17]. Since multiple solitons with different central frequencies emit radiation at distinct frequency intervals, a very large spectral range is covered. Subsequent experimental studies [5, 6, 7] by many groups provided evidence for this soliton-induced mechanism for SC generation.

Supercontinuum spectra from PCFs are 10^6 times brighter than sunlight ($\sim 10^3$ W/cm²/sterad) and have the same bandwidth. Unfortunately, the small radii in PCFs and material damage at few TW/cm² limit severely the maximum peak power densities to tens of W/nm. In this Letter we propose and study a novel approach for supercontinuum generation in metallic hollow waveguides coated with a dielectric. We predict that in such waveguides two-octave broad SC with up to five orders of magnitude higher spectral peak power densities than in PCFs can be generated. We also predict the generation of UV/VUV supercontinua in the range from 160 to 540 nm from such type of waveguide, a spectral range which can not be achieved by the previously used methods but which is of particular importance in many applications. The key idea in this approach is to use a hollow-core metal-dielectric waveguide filled with a noble gas instead of the solid-core microstructure fibers to in-

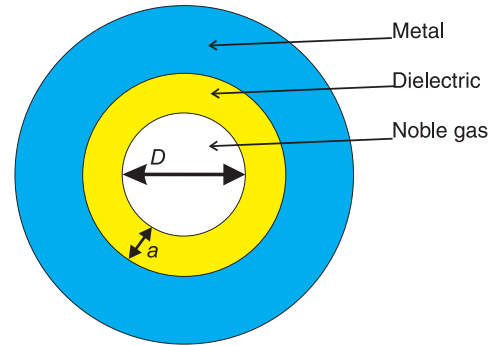


FIG. 1: Scheme of the hollow waveguide for supercontinuum generation.

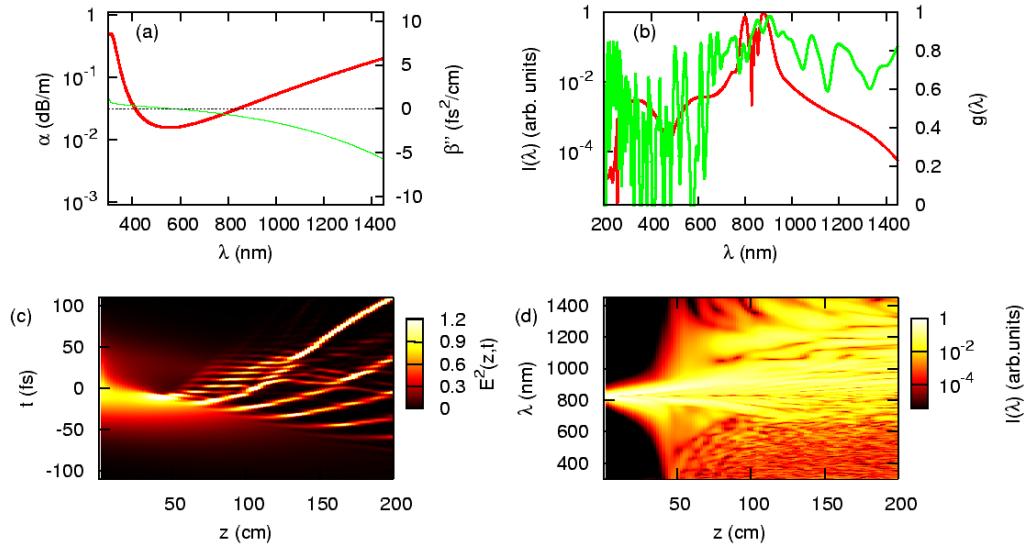


FIG. 2: High-power supercontinuum generation. Waveguide characteristics (a), generated output supercontinuum (red) and first-order coherence (green) (b), and evolution of temporal shape (c) and spectrum (d) in a $D = 80 \mu\text{m}$ silver waveguide coated with a 45-nm layer of fused silica and filled with argon at 1 atm. The input 100-fs pulse at 800 nm has the intensity of $50 \text{ TW}/\text{cm}^2$. In (a), loss (red) and group velocity dispersion (green) are presented. The roughness size σ equals 100 nm. The spectrum in (b) is presented after 50-cm propagation.

crease the diameter to a range between 20 to $80 \mu\text{m}$ and the damage threshold. The introduction of such waveguides has the aim to fulfill the conditions of small loss and anomalous dispersion at optical frequencies which are the basic requirements for the soliton-induced mechanism of supercontinuum generation, similar to the situation in microstructure fibers [4]. In recent years the application of standard dielectric hollow waveguides has led to impressive progress in ultrafast optics such as the generation of few-cycle [18] and attosecond pulses [19] and high-order harmonics [20]. However, these waveguides can not be used for the purpose studied here, because anomalous dispersion at optical frequencies and high pressures can only be achieved for small diameters in the range of 20- $80 \mu\text{m}$, for which the loss is too high.

Dielectric-coated metallic hollow waveguides can be produced by chemical vapor deposition [21, 22]. In Fig. 1, the geometry of such waveguide is presented. The hollow core of the fibre with diameter D is surrounded by a metallic cladding (blue) coated by a dielectric material such as silica (yellow) with thickness a on the inner side.

For the numerical simulations we use a generalized model based on the propagation equation for forward-going waves [4] with inclusion of higher-order transverse modes and the effects of ionization and plasma formation in the waveguide. The Fourier transform $\vec{E}(z, x, y, \omega)$ of the electromagnetic field $\vec{E}(z, x, y, t)$ in the waveguide can be represented by $\vec{E}(z, x, y, \omega) = \sum_j E_j(z, \omega) F_j(r, \omega)$, where $F_j(r, \omega)$ is the transverse mode profiles of the j -th mode and $E_j(z, \omega)$ describes the evolution of field with propagation. The inclusion of

higher-order transverse modes takes into account a possible energy transfer to higher-order modes by the non-linear polarization. We consider only linearly-polarized fields and therefore only EH_{1j} modes with the same polarization. The following first-order differential equation can be written for $E_j(z, \omega)$ in the EH_{1j} mode [4]:

$$\frac{\partial E_j(z, \omega)}{\partial z} = i\beta_j(\omega)E_j(z, \omega) - \frac{\alpha_j}{2}(\omega)E_j(z, \omega) + \frac{i\omega^2}{2c^2\epsilon_0\beta_j(\omega)}P_{NL}^{(j)}(z, \omega) \quad (1)$$

where $\beta_j(\omega)$ and $\alpha_j(\omega)$ are the wavenumber and the loss. This equation neglects backward-propagating components and contains only the first-order derivative over the propagation coordinate, but in difference to the non-linear Schrödinger equation (NSE) it does not rely on the slowly-varying envelope approximation and refer to the field components $E_j(z, \omega)$ and not to the amplitudes of the field. This approach allows to model the evolution of fs pulses with extremely broad spectra. The quantities $\beta_j(\omega)$, $\alpha_j(\omega)$ and $F_j(r, \omega)$ are calculated by the transfer-matrix approach assuming a circular waveguide structure as shown in Fig. 1, including the bulk dispersion of argon. Additionally, roughness loss is included in the calculation of $\alpha_j(\omega)$ using the model of pointlike scatterers; for further details of the transfer matrix theory and roughness loss calculation, see Ref. [23].

The Fourier transform of the j th component of the

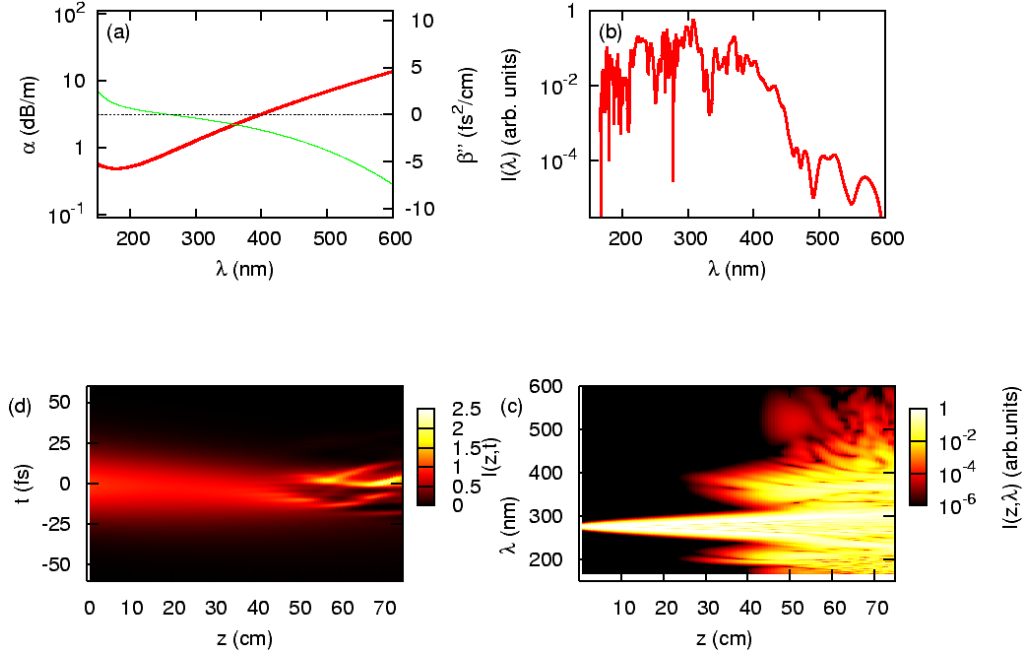


FIG. 3: UV/VUV supercontinuum generation. Waveguide characteristics (a), generated output supercontinuum (b), and evolution of the temporal shape (c) and spectrum (d) in a 20- μm aluminum waveguide with a 10-nm coating and filled with argon at 0.5 atm. The input 50-fs pulse at 266 nm has the input intensity of 40 TW/cm². In (a), loss (red) and group velocity dispersion (green) are presented.

nonlinear polarization $P_{NL}^{(j)}(z, \omega)$ is given by

$$P_{NL}^{(j)}(z, \omega) = \int_0^R 2\pi r F_j(r, \omega) \int_{-\infty}^{\infty} \exp(i\omega t) P_{NL}(z, r, t) dr dt \quad (2)$$

Here $P_{NL}(z, r, t)$ includes the Kerr nonlinearity, the plasma-induced refractive index change and absorption of light energy due to ionization. A theoretical description of light propagation in gases in the presence of photoionization and plasma can be found in numerous papers (see e.g. Ref. [24]). Taking these effects into account we can write for $P_{NL}(z, r, t)$:

$$P_{NL}(z, r, t) = \epsilon_0 \chi_3 E^3(z, r, t) - \rho(z, r, t) e d(z, r, t) - E_g \epsilon_0 c \int_{-\infty}^t \frac{E(z, r, t)}{\bar{I}(z, r, t)} \frac{\partial \rho(z, r, t)}{\partial t} dt \quad (3)$$

where $\chi_3 = (4/3)c\epsilon_0 n_2$ is the third-order polarizability of the gas filling and $\bar{I}(z, r, t)$ is the intensity averaged over few optical periods. For argon we have $n_2 = 1 \times 10^{-19} \text{ cm}^2/\text{W}$ at 1 atm, $E_g = 15.95 \text{ eV}$ is the ionization potential, $\rho(z, r, t)$ is the electron density and $d(z, r, t)$ is the mean free-electron displacement in the electric field. The evolution of the two latter quantities is described by

$$\frac{\partial \rho(z, r, t)}{\partial t} = (N_0 - \rho(z, r, t)) \Gamma(\bar{I}(z, r, t)) \quad (4)$$

$$\frac{\partial^2 d(z, r, t)}{\partial t^2} = -e E(z, r, t) / m_e \quad (5)$$

where $\Gamma(\bar{I}(z, r, t))$ is the photoionization rate calculated from the Faisal-Reiss-Keldysh model[25] which describes both the multiphoton and tunnelling regime and N_0 is the initial argon density. The coherence properties of the supercontinua [10, 11] are described by the first-order coherence function $g(\lambda)$ defined as

$$g(\lambda) = \Re \left[\frac{\langle E_b(\lambda) E_a^*(\lambda) \rangle_{ab, a \neq b}}{\langle E_a(\lambda) E_a^*(\lambda) \rangle_a} \right] \quad (6)$$

where the indices a, b denote the different input realizations and $E_a(\lambda)$ is the spectrum for the realisation a . Pulse evolution with propagation is modelled for each realisation of the input quantum shot noise, which is added to the input pulse. These realisations are implemented as described in Ref. [11]. Equations (1)-(5) are solved by the split-step Fourier method with Runge-Kutta nonlinear steps.

First we study the loss and dispersion properties of a silver waveguide with a diameter of 80 μm coated from the inner side with a 45nm layer from fused silica. In Fig. 2(a) can be seen that the loss remains relatively low in the range of 10^{-2} - 10^{-1} dB/m for wavelengths from 0.4 μm to 1.4 μm . This means that at most 10% of the energy is lost during a propagation over 1 m, while in a conventional dielectric hollow waveguide with the same diameter, roughly 80% of the energy is lost. The physical reason for this difference is that the reflection coefficient for grazing incidence of light is higher for fused-silica-coated silver than for a layer of fused silica. The increased

transmission of dielectric-coated metallic waveguides allow a reduction of the diameter of the waveguides while keeping the losses acceptable. This, in turn, leads to significant modification of the dispersion properties and an extended range of anomalous dispersion[23]. The group velocity dispersion, illustrated in Fig. 2(a) by the green curve, is anomalous for $\lambda > 570$ nm at 1 atm of the argon filling.

The optical properties of the studied waveguide as illustrated in Fig. 2(a) allows the conjecture that soliton-induced supercontinuum generation can be generated in such waveguide. To study this question we consider the evolution of a 100-fs input pulse at 830 nm with a peak intensity of 50 TW/cm² propagating a maximum distance of 2 m in the above-described fiber with 10 modes included in the simulation. We assume that the input field is completely in the EH₁₁ mode, but during propagation roughly 20% of energy is transferred to higher-order modes. It can be seen in Fig. 2(b) that the generated radiation cover the spectral range from 250 nm to 1200 nm, with a total width corresponding to more than two octaves. This supercontinuum is generated already after 50 cm of propagation, as shown in Fig. 2(d). In Fig. 2(b) the first-order coherence is shown by the green curve demonstrating a high average value of 0.92. The supercontinuum generation is stable against manufacturing imperfections and variation of input pulse parameters. The energy fraction in the cladding is around 10⁻³, which guarantees that it is not damaged. The wavelength-averaged peak power spectral density is about 10⁶ W/nm with an intensity at the output of about 10¹⁴ W/cm². The obtained spectral power density is 10⁵ times higher than in standard PCFs. For comparison, the Sun at its surface has a brightness of 10³ W/cm²/sterad, which is roughly 10¹¹ times lower than the results predicted here. The temporal shape presented in Fig. 2(c) shows that the pulse is split into many solitons and background radiation which move with different velocities. The supercontinuum is explained by the same mechanism as in photonic crystal fibres due to the emission of nonsoliton radiation by several frequency-shifted solitons[4].

Supercontinua from PCFs have the shortest wavelengths in the ultraviolet at about 300 nm. There exists a strong interest in molecular physics and material science in extending the achievable spectrum still further towards the vacuum ultraviolet (VUV). Here we show that dielectric-coated metallic hollow waveguides can also be used for this purpose and predict a high-power VUV supercontinuum source, which is based on an appropriately designed fused-silica-coated aluminium waveguides filled with argon.

We consider an optimized aluminum waveguide with the diameter of only 20 μ m coated by a 10-nm layer of fused-silica. The linear optical properties of this waveguide are shown in Fig. 3(a), demonstrating moderate loss and anomalous dispersion for $\lambda > 260$ nm at 1 atm.

In Fig. 3(b)-(d) the generation of an ultraviolet/vacuum ultraviolet supercontinuum from a third harmonic pulse of a Ti:sapphire amplifier laser system with input pulses at 266 nm and intensity of 40 TW/cm² is illustrated. The evolution of spectra (d) and the temporal shape (c) demonstrates an initial generation of two side peaks by four-wave mixing followed by fission into several solitons and soliton emission. The output spectrum reaches from 160 to 540 nm, as shown by the red curve in Fig. 3(b).

In conclusion, we studied the generation of high-power supercontinua in specially designed metallic dielectric coated waveguides. We predicted that supercontinua with two-octave width, spectral power densities in the range of MW/nm five orders of magnitude higher than in microstructured fibers, and high coherence, can be achieved in such waveguides. Additionally, we predicted the generation of UV/VUV supercontinuum in an aluminum hollow waveguide.

The findings that we report could have applications in a wide range of fields. Let us remark just a few. In combination with a multichannel frequency filter the high- power SC source can replace many lasers at separated frequencies including wavelengths where lasers are not available (as e.g. in the UV/VUV). The predicted VUV supercontinuum could lead to advances in VUV frequency comb spectroscopy [26]. Further on, direct difference frequency mixing of two portions of the SC [27] eliminates the carrier-offset frequency and its noise which can be used in frequency metrology. The detection sensitivity of nonlinear spectroscopic methods such as CARS microscopy [28] can be significantly increased by an increase of the CS intensity.

* Electronic address: [gusakov@mbi-berlin.de

- [1] J. C. Knight *et al.*, *Opt. Lett.* **21**, 1547 (1996).
- [2] P. Russel, *Science* **299**, 358 (2003).
- [3] J. K. Ranka, R. S. Windeler, and A. J. Stentz, *Opt. Lett.* **25**, 25 (2000).
- [4] A. V. Husakou and J. Herrmann, *Phys. Rev. Lett.* **87**, 203901 (2001).
- [5] J. Herrmann *et al.*, *Phys. Rev. Lett.* **88**, 173901 (2002).
- [6] A. Ortigosa-Blanch, J. C. Knight, and P. St. J. Russel, *J. Opt. Soc. Am. B* **19**, 2567 (2002).
- [7] J. Dudley *et al.*, *Opt. Express* **10**, 1215 (2002)
- [8] A. L. Gaeta, *Opt. Lett.* **27**, 924 (2002).
- [9] K. L. Corwin *et al.*, *Phys. Rev. Lett.* **90**, 113904 (2003).
- [10] J. M. Dudley *et al.*, *Rev. Mod. Phys.* **78**, 1135 (2006).
- [11] D. TÜRKE *et al.*, *Opt. Express* **15**, 2732 (2007).
- [12] D. J. Jones *et al.*, *Science* **288**, 635 (2000).
- [13] R. Holzwarth *et al.*, *Phys. Rev. Lett.* **85**, 2264 (2000).
- [14] I. Hartl *et al.*, *Opt. Lett.* **26**, 608 (2001).
- [15] J. Swartling *et al.*, *Appl. Optics* **44**, 4684 (2005).
- [16] H. Imam, *Nature Photonics* **2**, 26 (2008).
- [17] N. Akhmediev and M. Karlsson, *Phys. Rev. A* **51**, 2602 (1995).
- [18] M. Nisoli *et al.*, *Opt. Lett.* **22**, 522 (1997).

- [19] M. Drescher *et al.*, Science **291**, 1923 (2001).
- [20] A. Rundquist *et al.*, Science **280**, 1412 (1998).
- [21] Y. Matsuura and J. A. Harrington, Opt. Lett. **20**, 2078 (1995).
- [22] P. J. A. Sazio *et al.*, Science **311**, 1583 (2006).
- [23] A. Husakou and J. Herrmann, Opt. Express **16**, 3834 (2008).
- [24] P. Sprangle, J. R. Penano, B. Hafizi, and C. Kapetanacos, Phys. Rev. E **69**, 066415 (2004).
- [25] H. R. Reiss, Phys. Rev. A **22**, 1786 (1980).
- [26] R. J. Jones *et al.*, Phys. Rev. Lett. **94**, 193201 (2005).
- [27] A. Baltuška *et al.*, Phys. Rev. Lett. **88**, 133901 (2002).
- [28] H. N. Paulsen *et al.*, Opt. Lett. **28**, 1123 (2003).